

---

# Princeton Plasma Physics Laboratory

---

PPPL-

PPPL-



Prepared for the U.S. Department of Energy under Contract DE-AC02-09CH11466.

# Princeton Plasma Physics Laboratory

## Report Disclaimers

---

### Full Legal Disclaimer

This report was prepared as an account of work sponsored by an agency of the United States Government. Neither the United States Government nor any agency thereof, nor any of their employees, nor any of their contractors, subcontractors or their employees, makes any warranty, express or implied, or assumes any legal liability or responsibility for the accuracy, completeness, or any third party's use or the results of such use of any information, apparatus, product, or process disclosed, or represents that its use would not infringe privately owned rights. Reference herein to any specific commercial product, process, or service by trade name, trademark, manufacturer, or otherwise, does not necessarily constitute or imply its endorsement, recommendation, or favoring by the United States Government or any agency thereof or its contractors or subcontractors. The views and opinions of authors expressed herein do not necessarily state or reflect those of the United States Government or any agency thereof.

### Trademark Disclaimer

Reference herein to any specific commercial product, process, or service by trade name, trademark, manufacturer, or otherwise, does not necessarily constitute or imply its endorsement, recommendation, or favoring by the United States Government or any agency thereof or its contractors or subcontractors.

---

## PPPL Report Availability

### Princeton Plasma Physics Laboratory:

<http://www.pppl.gov/techreports.cfm>

### Office of Scientific and Technical Information (OSTI):

<http://www.osti.gov/bridge>

---

### Related Links:

[U.S. Department of Energy](#)

[Office of Scientific and Technical Information](#)

[Fusion Links](#)

# Optimization of the configuration of pixilated detectors based on the Shannon-Nyquist theory for the x-ray spectroscopy of hot tokamak plasmas<sup>a)</sup>

E. Wang<sup>1</sup>, P. Beiersdorfer<sup>1</sup>, M. Bitter<sup>2</sup>, L. F. Delgado-Aparicio<sup>2</sup>, K. W. Hill<sup>2</sup>,  
and N. Pablant<sup>2</sup>

<sup>1</sup>Lawrence Livermore National Laboratory, Livermore, CA 94550, USA

<sup>2</sup>Princeton Plasma Physics Laboratory, Princeton, New Jersey 08543, USA

(Presented XXXXX; received XXXXX; accepted XXXXX; published online XXXXX)

(Dates appearing here are provided by the Editorial Office)

This paper describes an optimization of the detector configuration, based on the Shannon-Nyquist theory, for two major x-ray diagnostic systems on tokamaks and stellarators: x-ray imaging crystal spectrometers and x-ray pinhole cameras. Typically, the spectral data recorded with pixilated detectors are oversampled, meaning that the same spectral information could be obtained using fewer pixels. Using experimental data from Alcator C-Mod, we quantify the degree of oversampling and propose alternate uses for the redundant pixels for additional diagnostic applications.

## I. INTRODUCTION

In this paper, we use the Shannon-Nyquist theory to optimize the configurations of pixilated detectors for two main x-ray diagnostics of tokamak plasmas, the x-ray imaging crystal spectrometers and pinhole cameras, which are used for measurements of ion temperature profiles and profiles of the x-ray continuum, respectively. The Shannon-Nyquist theory was originally developed for signal processing, and makes the following statements:

(1) A signal  $s(t)$ , which is a continuous function of time  $t$ , can be uniquely reconstructed at any time  $t$  from a sequence of discrete samples  $s_n = s(nT_s)$ , taken in constant time intervals  $T_s$ , if the sampling frequency  $f_s = 1/T_s$  is larger than twice the bandwidth or the maximum characteristic frequency  $f_{\max}$  of the signal,

$$f_s = 2f_{\max}. \quad (1)$$

(2) If the condition (1) is satisfied, the signal  $s(t)$  can be reconstructed exactly, using the Whittaker-Shannon interpolation formula:

$$s(t) = \sum_{n=0}^{N-1} s(nT_s) \frac{\sin[\pi(t/T_s - n)]}{\pi(t/T_s - n)}. \quad (2)$$

To optimize the detector configuration for the above-mentioned diagnostics, we consider the number of photon counts per pixel as samples of a continuous function of  $x$ , where  $x$  is the pixel coordinate on the detector, and we ask the question ‘How many pixels are needed to reconstruct the observed spectra?’ As will be demonstrated, the underlying spectra are typically oversampled. Therefore pixels can be skipped because they contain redundant information, and used for other purposes.

## II. OPTIMIZED DETECTOR CONFIGURATIONS

### A. X-ray Imaging Crystal Spectrometers

X-ray imaging crystal spectrometers are now widely used for measurements of profiles of the ion temperature and

profiles of the flow velocities in hot tokamak and stellarator plasmas<sup>1-5</sup>. Here, the ion temperature and flow velocities are determined from the Doppler broadening and Doppler shifts of x-ray  $K\alpha$ -lines of highly charged impurity ions, such as  $\text{Ar}^{16+}$ ,  $\text{Fe}^{24+}$ , or  $\text{Kr}^{34+}$ , in the x-ray energy range from 3 to 13 keV. As required for Doppler measurements, the spectral resolution of these imaging crystal spectrometers is of the order of  $\lambda/\Delta\lambda = 10,000$ . However, the spectral resolution and dispersion,  $\Delta\lambda/\Delta x$ , where  $x$  is the detector coordinate, vary from instrument to instrument, since the spectrometer designs on different machines are adapted to varying experimental constraints. Thus, the same spectral line is recorded on LHD<sup>5</sup> with four times as many pixels as on Alcator C-Mod<sup>1</sup>; both spectrometers record the spectrum of He-like argon,  $\text{Ar}^{16+}$ , in the wavelength range from 3.9494 to 3.9944 Å with a pixilated (100K Pilatus II) detector<sup>6</sup>. Therefore, the question arises as to how many pixels are needed for the measurement of a Doppler broadened spectral line.

Figure 1a) shows a spectrum of  $\text{Ar}^{16+}$  from Alcator C-Mod shot 1078030010, recorded with the x-ray imaging crystal spectrometer on a Pilatus detector, with a pixel size of 172 μm and a sensitive area of 83.8 x 33.5 mm<sup>2</sup>. The short (33.5 mm) dimension of the detector was used to display spectral (wavelength) information, while the long (83.8 mm) dimension was used to display spatial information in the plasma. The experimental data (blue crosses) shown in Fig. 1a) represent a spectrum from a central sightline through the plasma. This spectrum was recorded on the central 12 pixel rows on the detector during a time interval of 100 ms. The black line shown in Fig. 1a) presents the Whittaker-Shannon interpolation, given by Equation 2, using each data point. The interpolation was calculated on a one-micron scale, so that one obtains 172 points per pixel. By definition, the Whittaker-Shannon interpolation curve passes through each of the  $N$  data points which are used in Equation 2.

Figure 1b) shows an overlay of three Whittaker-Shannon interpolation curves obtained using every data point (black), every other point (blue) and every third point (red). Except for very small deviations, which are further discussed

<sup>a)</sup>Contributed paper published as part of the Proceedings of the 19th Topical Conference on High-Temperature Plasma Diagnostics, Monterey, California, May, 2012.

<sup>b)</sup>Author to whom correspondence should be addressed: ericwang1980@gmail.com

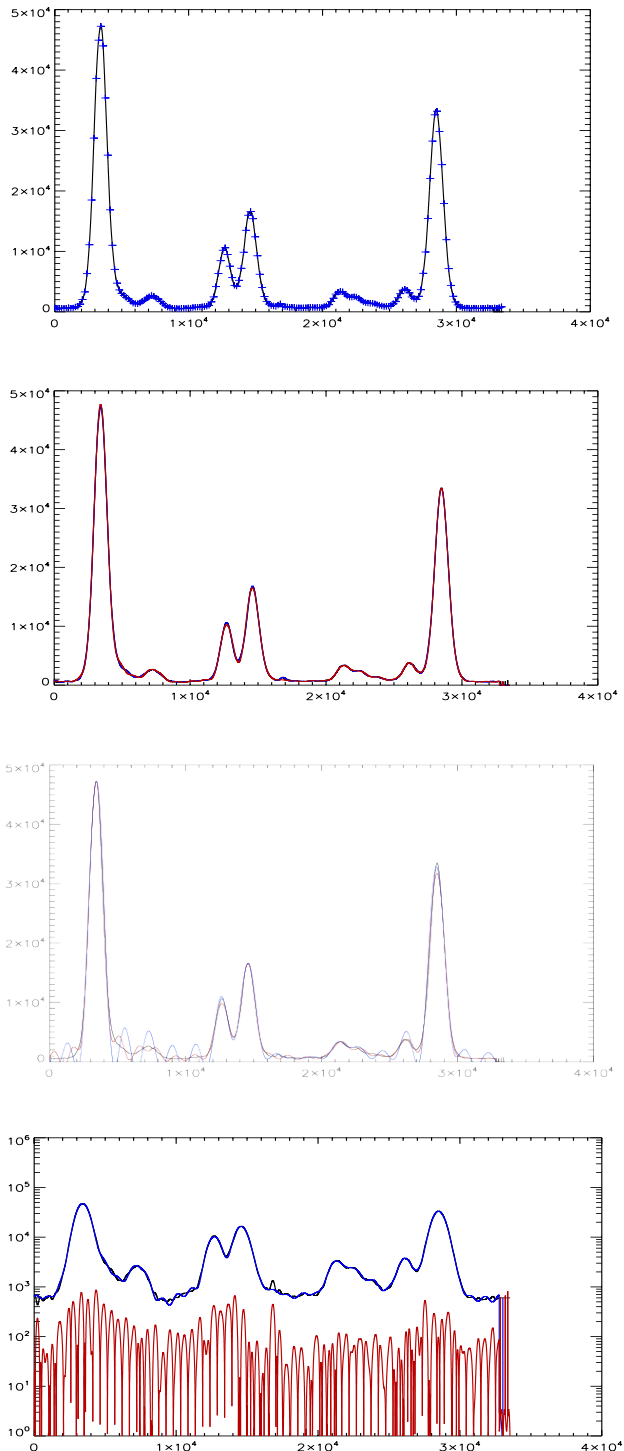


FIG. 1. Spectral data of He-like Ar from Alcator C-Mod (blue cross) and Whittaker-Shannon interpolation curves on a one-micron scale. Different colors denote interpolations obtained for different sets of pixels, as described in text.

below, the three curves are in excellent agreement, indicating that the Shannon-Nyquist sampling theorem of Equation 1 is satisfied for all curves. By contrast, Fig. 1c) shows an overlay of the black curve from Fig. 1a) with Whittaker-Shannon interpolation curves obtained by using every fourth (red) and fifth (blue) data point. It is obvious from Fig. 1c) that the red and blue curves differ

significantly from the black curve, indicating that the Shannon-Nyquist condition, given by Equation 1, is no longer satisfied, so that distortions occur due to aliasing because the “sampling frequency” obtained by using only every 4<sup>th</sup> or 5<sup>th</sup> is less than twice the “bandwidth” of the spectrum. The very small deviations of the red and blue curves from the black curve, which are barely noticeable in Fig. 1b), cannot be ascribed to aliasing. These deviations are due to the fact that different sets of data points were used for the construction of the black, red, and blue curves. Since these different sets of data points are experimental points with statistical errors, they are, strictly speaking, not equivalent. Figure 1d) shows again an overlay of the black and blue Whittaker-Shannon interpolation curves from Fig. 1b) on a logarithmic scale to emphasize the differences between these two curves; the absolute amount of these differences is shown by the red curve in Fig. 1d). We infer from Fig. 1d) that the differences between black and blue curves are of the order of 100 photon counts or about 1% of the number  $N \approx 10,000$  of photon counts per pixel at the peak of a spectral line. The differences between the black and blue curves are, therefore, comparable to the statistical error,  $N^{1/2}$ , of the experimental data. We conclude from this discussion that the spectrum shown in Fig. 1a) can be reliably reconstructed from Whittaker-Shannon interpolation formula by using only every second or every third pixel.

The pixels skipped can therefore be used for other purposes. For instance, the spectra of He-like argon,  $\text{Ar}^{16+}$ , He-like titanium  $\text{Ti}^{20+}$ , and He-like iron,  $\text{Fe}^{24+}$ , at x-ray energies of 3.1keV, 4.75keV, and 6.7keV, respectively, could be simultaneously recorded on the same detector by sequentially setting the energy thresholds of three adjacent columns of pixels appropriately for the above-mentioned x-ray energy values. To evaluate these spectral data from the so-configured detector, one would proceed as follows:

In a first step, one would reconstruct the spectrum of He-like iron from the Whittaker-Shannon interpolation formula, using the pixels with the highest threshold, and subtract the photon counts due to He-like iron from the adjacent pixels, which are set at lower energy thresholds and which are dedicated to record the spectra of  $\text{Ti}^{20+}$  and  $\text{Ar}^{16+}$ . In a second step, one would reconstruct the spectrum of  $\text{Ti}^{20+}$  and correct the photon counts in the pixels dedicated to  $\text{Ar}^{16+}$ ; and in the third and final step, one would then reconstruct the spectrum of  $\text{Ar}^{16+}$  from the pixels with the lowest energy threshold.

The above-described optimization of the detector configuration has significant advantages.

## B. Pinhole Cameras

As a second example we discuss detector configurations for a new x-ray pinhole camera<sup>7</sup>, which will be used on tokamaks for profile measurements of the x-ray continuum. A schematic of the experimental arrangement is shown in Fig. 2. Here, the toroidal magnetic field is perpendicular to the drawing plane, and the orientation of the pixilated detector, a Pilatus 100K detector<sup>6</sup>, is such that the rows of pixels in the short (33.5 mm) dimension of the detector and the columns of pixels in the long (83.8 mm) dimension are, respectively, parallel and perpendicular to the toroidal magnetic field. With this experimental arrangement, the pixels in the same row are mapped to different points along the toroidal magnetic field but record the same information since the electron density, electron temperature, and therefore the x-ray emissivity are uniform along the toroidal magnetic field. It is

therefore possible to obtain spectral resolution by setting the pixels in one row to different energy thresholds,  $E_1, E_2, E_3, E_4$ , etc., as shown in Fig. 2b), where a larger number of pixels is assigned to the higher energy threshold  $E_4$  and a smaller number of pixels with the lower energy threshold  $E_1$  to compensate for the exponential decrease in photon intensity with energy. The configuration shown in Fig. 2b) is however not optimal. The optimized configuration, according to Shannon-Nyquist theory, is shown in Fig. 2c).

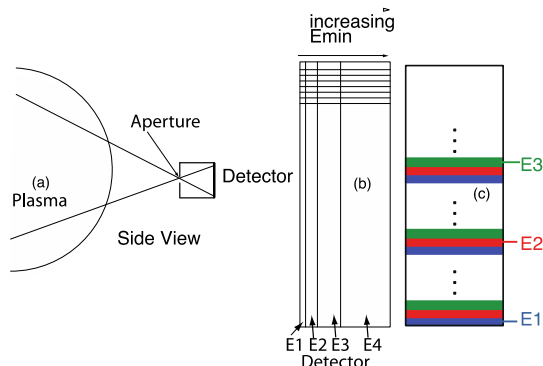


FIG. 2. Pinhole camera to measure profiles of the x-ray continuum on a tokamak experiment (a) and two possible detector configurations (b,c) where configuration (c) is based on the Shannon-Nyquist theory.

Figure 3 shows a two-dimensional profile of the x-ray continuum from Alcator C-Mod measured with the new pinhole camera<sup>7</sup>, where all pixels have been set to the same energy threshold,  $E$ . As expected, the profiles are fairly uniform in the x-direction on the detector, which is parallel to the toroidal magnetic field. In the z-direction, which is perpendicular to the toroidal magnetic field, the profile is broad and smooth, suggesting that much fewer pixels are necessary to reliably measure this profile. In fact, as shown in Fig. 4, it is possible to obtain the same profile with a detector configuration optimized according to the scheme shown in Fig. 2c) if only every 20<sup>th</sup> row of pixels is being used with energy threshold  $E$ . As a result, the other 19 skipped rows of pixels can be set to different energy thresholds with no loss of information, allowing for an improved spectral resolution with 20 discrete energy values. An additional advantage of the configuration (c) over configuration (b) in Fig. 2 is that effectively the entire detector area is used for every energy value because, by skipping pixels, only redundant information is discarded. By contrast, the configuration (b) uses only a fraction of the detector area for each energy.

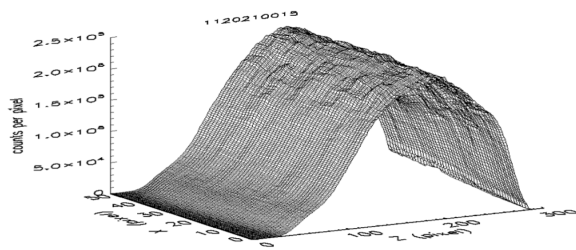


Fig. 3. Profile of x-ray continuum measured with a pinhole camera on Alcator C-Mod. All pixels are set for the same energy threshold. The x-direction on the detector is parallel and the z-direction is perpendicular to the toroidal magnetic field.

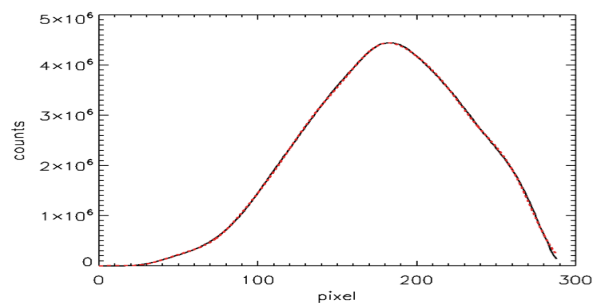


Fig. 4. Profile of x-ray continuum obtained from Fig. 3 by summing over the x-direction (parallel to the toroidal magnetic field) and using Whittaker-Shannon interpolation between every pixel (black curve) or every 20<sup>th</sup> pixel (red curve) on a one-micron scale.

## ACKNOWLEDGMENTS

This work was performed under the auspices of the U.S. DOE by LLNL under Contract No. DE-AC52-07NA-27344. LLNL-JRNL-555431

## REFERENCES

- <sup>1</sup>A. Ince-Cushman, J. E. Rice, M. Bitter, M. L. Reinke, K. W. Hill, M. F. Gu, E. Eikenberry, Ch. Broennimann, S. Scott, Y. Podpaly, S. G. Lee, and E. S. Marmor, *Rev. Sci. Instrum.* **79** 10E302 (2008)
- <sup>2</sup>S. G. Lee<sup>1</sup>, J. G. Bak<sup>1</sup>, U. W. Nam<sup>2</sup>, M. K. Moon<sup>3</sup>, Y. Shi<sup>4</sup>, M. Bitter<sup>5</sup>, and K. Hill, *Rev. Sci. Instrum.* **81** 10E506 (2010)
- <sup>3</sup>Yuejiang Shi, Fudi Wang, Baonian Wan, Manfred Bitter, Sanggon Lee, Jungyo Bak, Kenneth Hill, Jia Fu, Yingying Li, Wei Zhang, Ang Ti and Bili Ling, *Plasma Phys. Control. Fusion.* **52** 085014 (2010)
- <sup>4</sup>N. Pablant, M. Bitter, L. Delgado-Aparicio, K. Hill, S. Lazerson, L. Roquemore, D. Gates, D. Monticello, H. Neilson, A. Reiman, M. Goto, S. Morita, H. Yamada, M. Reinke, J. Rice, 53rd Annual Meeting of the APS Division of Plasma Physics (2011)
- <sup>5</sup>M. Bitter, K. Hill, D. Gates, D. Monticello, H. Neilson, A. Reiman, A. L. Roquemore, S. Morita, M. Goto, H. Yamada, and J. E. Rice, *Rev. Sci. Instrum.* **81**, 10E328 2010
- <sup>6</sup>DECTRIS / Next Generation X-ray Detectors: <http://www.dectris.com/pilatus-100k.html>
- <sup>7</sup>K. W. Hill, *et al.*, 53<sup>rd</sup> Annual Meeting of the APS Division of Plasma Physics, November 14-18, 2011, Salt Lake City, Utah, **TP9 143**

The Princeton Plasma Physics Laboratory is operated  
by Princeton University under contract  
with the U.S. Department of Energy.

Information Services  
Princeton Plasma Physics Laboratory  
P.O. Box 451  
Princeton, NJ 08543

Phone: 609-243-2245  
Fax: 609-243-2751  
e-mail: [pppl\\_info@pppl.gov](mailto:pppl_info@pppl.gov)  
Internet Address: <http://www.pppl.gov>